Examining the West African Monsoon circulation response to atmospheric heating in a GCM dynamical core

Robin E. Chadwick, Gill Martin, Dan Copsey, Gilles Bellon, M. Caian, Francis Codron, Catherine Rio, Romain Roehrig

AGU PUBLICATIONS

Journal of Advances in Modeling Earth Systems

RESEARCH ARTICLE

10.1002/2016MS000728

Examining the West African Monsoon circulation response to atmospheric heating in a GCM dynamical core

R. Chadwick [1], G.M. Martin [1], D. Copsey [1], G. Bellon [2,3], M. Caian[4], F. Codron [2], C. Rio[2], and R. Roehrig [5]

[1]Met Office, Exeter, UK, [2]Laboratoire de Météorologie Dynamique, Institut Pierre-Simon Laplace, Paris, France, [3]Now at Department of Physics, University of Auckland, New Zealand, [4]Swedish Meteorological and Hydrological Institute, Norrköping, Sweden, [5]Centre National de Recherches Météorologiques, Météo-France, Toulouse, France

Key Points:
- The main features of the West African monsoon flow can be reproduced in a dynamical core
- Atmospheric shortwave absorption over the Sahara and Sahel is a major driver of differences between models.
- A dynamical core can be used to understand circulation changes in relation to model development.

Correspondence to:
R. Chadwick,
robin.chadwick@metoffice.gov.uk

Citation:
Chadwick, R., G. M. Martin, D. Copsey, G. Bellon, M. Caian, F. Codron, C. Rio, and R. Roehrig (2017), Examining the West African Monsoon circulation response to atmospheric heating in a GCM dynamical core, *J. Adv. Model. Earth Syst.*, *9*, doi:10.1002/2016MS000728.

Received 2 JUN 2016
Accepted 9 AUG 2016
Accepted article online 20 DEC 2016

Abstract Diabatic heating plays a crucial role in the formation and maintenance of the West African Monsoon. A dynamical core configuration of a General Circulation Model (GCM) is used to test the influence of diabatic heating from different sources and regions on the strength and northward penetration of the monsoon circulation. The dynamical core is able to capture the main features of the monsoon flow, and when forced with heating tendencies from various different GCMs it recreates many of the differences seen between the full GCM monsoon circulations. Differences in atmospheric short-wave absorption over the Sahara and Sahel regions are a key driver of variation in the models' monsoon circulations, and this is likely to be linked to how aerosols, clouds and surface albedo are represented across the models. The magnitude of short-wave absorption also appears to affect the strength and position of the African easterly jet (AEJ), but not that of the tropical easterly jet (TEJ). The dynamical core is also used here to understand circulation changes that occur during the ongoing model development process that occurs at each modeling centre, providing the potential to trace these changes to specific alterations in model physics.

1. Introduction

The West African Monsoon (WAM) is the main source of rainfall for many millions of people and is responsible for large seasonal changes in weather over the region. However, despite substantial recent research efforts and improvements in physical understanding of the monsoon circulation [e.g., *Redelsperger et al.*, 2006; *Lafore et al.*, 2011; *Nicholson*, 2013; *Roehrig et al.*, 2013], it remains inadequately represented in the majority of climate models [e.g., *Hourdin et al.*, 2010; *Xue et al.*, 2010; *Roehrig et al.*, 2013]. Improved simulation of the monsoon circulation would increase confidence in predictions of seasonal rainfall amounts and monsoon onset date, crop growth, and Saharan/Sahelian dust uplift, in both seasonal-to-decadal forecasts and longer-term climate projections for the region.

Figure 1 shows the mean WAM circulation during August as represented by the ERA-Interim [*Simmons et al.*, 2007] reanalysis. Features of note which are not always well simulated in climate models include the low-level south-westerly monsoon flow, the heat-low circulation over the Sahara, the mid-level African Easterly Jet (AEJ), and the upper-level Tropical Easterly Jet (TEJ). The strength and position of these phenomena appear to be closely related to the position of the rain-band over West Africa during the monsoon season, though cause and effect are not yet fully understood [e.g., *Nicholson*, 2013].

Diabatic heating is a crucial driver of the tropical circulation [e.g., *Gill*, 1980; *Schumacher et al.*, 2004], and variations across climate models in the position and strength of diabatic heat sources is one likely reason for biases in their monsoon circulations. The differing magnitude and distribution of heating between the various models is related to choice of physical parametrizations. For example, "convective" and "stratiform" heating profiles [*Houze*, 1989], with maximum heating at mid and upper levels respectively, have been shown to produce different types of circulation [*Wu et al.*, 2000; *Dearden*, 2006], and boundary layer heating may also be an important driver of tropical convergence [*Lindzen and Nigam*, 1987; *Chiang et al.*, 2001; *Back and Bretherton*, 2009]. Contending influences from sources of latent and "nonlatent" heating have also been proposed to be influential on the position of the WAM rain-band [*Hagos and Zhang*, 2010].

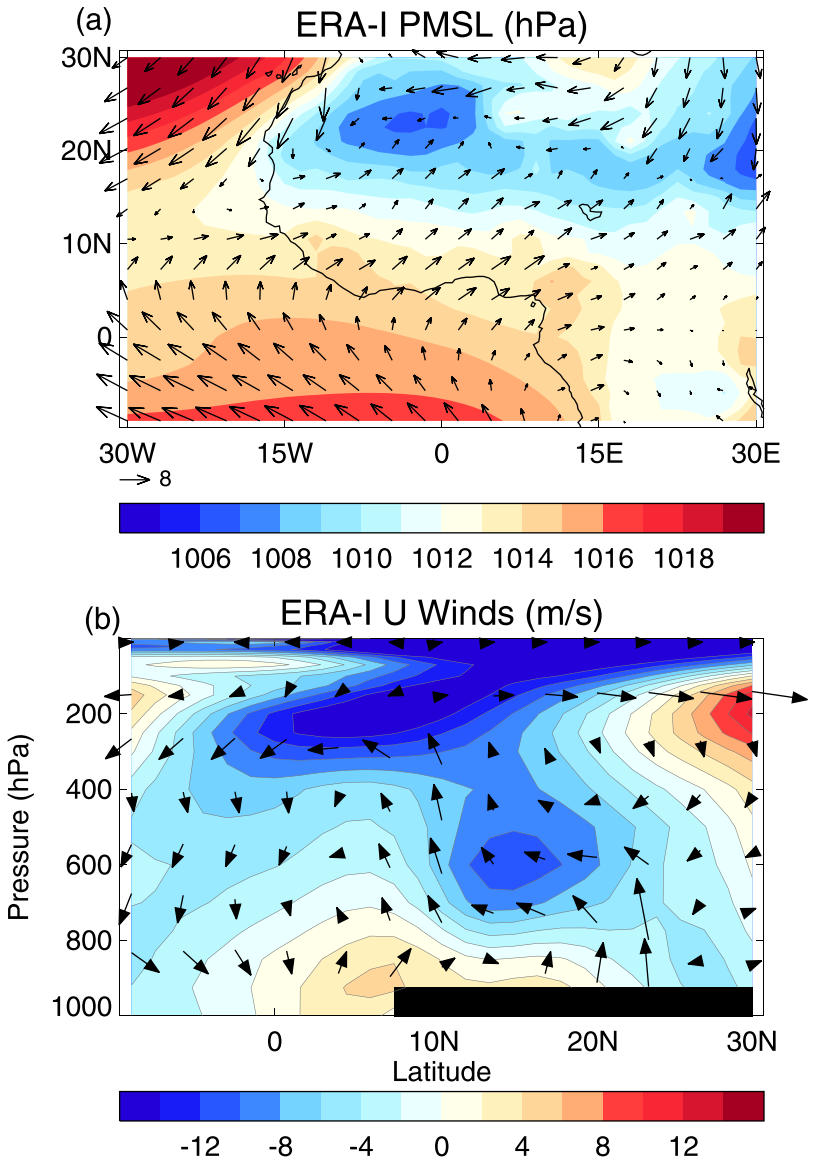

Figure 1. WAM in the ERA-Interim reanalysis: (a) Pressure at Mean Sea Level (PMSL) (colours, hPa) and 925 hPa winds (vectors, m/s). (b) Cross section (10W – 10E) of zonal winds (colours, m/s), with meridional and vertical winds shown as vectors. Mean August values for 1989–2008 are shown.

Martin et al. [2017] examined the relationship between diabatic heating and the WAM circulation in a selection of climate models from four model families (listed in Table 1), chosen because of their participation in the EMBRACE (Earth system Model Bias Reduction and assessing Abrupt Climate change) project. They were able to trace some differences between the monsoon circulations of various models to differences in their sources of diabatic heating, and potentially to more detailed aspects of their parametrizations. One conclusion was that the magnitude of atmospheric short-wave radiative absorption over the Sahara and Sahel regions appears to be an important determinant of the strength and northward penetration of the monsoon flow in GCMs.

Differences in atmospheric SW absorption between models could be due to their representation of surface albedo, clouds and dust or other aerosols, and their interactions with radiation over West Africa (*Martin et al.* [2017]). Saharan dust and its effect on atmospheric and surface absorption of radiation has previously been suggested to be influential on the monsoon circulation [*Konare et al.*, 2008, *Lau et al.*, 2009, *Zhao et al.*, 2011]. *Lau et al.* [2009] proposed that SW radiative absorption by dust drives the monsoon circulation in

Table 1. List of Model Experiments and Naming Conventions Used in This Study[a]

Centre	Model Configurations	Naming Conventions
CNRM, Meteo-France, Toulouse	ARPEGE-Climat V5.2, used in CMIP5	CNRM-AM5
	PreCNRM-AM6 (a development configuration)	PreCNRM-AM6
SMHI, Sweden	EC-Earth v2.3, used in CMIP5	EC-Earth v2.3
Met Office, UK	MetUM HadGEM2-A, used in CMIP5	HadGEM2-A
LMD, IPSL Paris	LMDZ5A, used in CMIP5	LMDZ5A
	LMDZ5B (used to produce a subset of CMIP5 simulations with IPSL-CM5B)	LMDZ5B
	NPv4.12.OR11 (a development configuration including changes motivated by other work in EMBRACE)	NPV4.12.OR11

[a]A detailed discussion of differences between the formulation of these models is presented in *Martin et al.* [2017].

two opposing ways, with reduced surface absorption weakening the monsoon flow, and increased atmospheric absorption (the "elevated heat pump") strengthening it. The precipitation response to dust radiative forcing is highly sensitive to both the concentration and the radiative properties of dust [*Konare et al*., 2008], so differences in dust across GCMs could potentially have a large influence on their representations of the WAM.

Here we describe the development and application of an idealized dynamical core modeling framework in which the mean circulation response to parametrized temperature increments can be tested, without the full range of processes and feedbacks contained in a GCM. We use this framework to test some of the hypotheses of *Martin et al.* [2017], with regard to the influence of diabatic heating from specific parametrizations, as well as diabatic heating in particular regions, on the monsoon circulation. In particular we test whether short-wave radiative absorption is an important contributor to differences between models.

We also examine some of the differences in monsoon circulation between different versions of two EMBRACE model families, and use the dynamical core to test the influence of diabatic heating within several monsoon subregions on these differences.

In section 2, we describe the concept of a dynamical core, and how the HadGEM2 dynamical core was modified and used to simulate the WAM, with the intention of understanding differences between the representation of the monsoon flow in the EMBRACE models. Section 3 describes the results of these simulations, and section 4 provides a summary and conclusions.

2. Methods

2.1. Dynamical Core

First proposed by *Held and Suarez* [1994], the dynamical core configuration of a GCM arises from considering a GCM as being composed of a series of modules that can be independently tested and compared with those from other GCMs. One such module is the dry atmospheric dynamics, with no humidity and no parametrizations of subgrid processes, and this is known as the dynamical core.

Dynamical core experiments are generally constructed with a "relaxation" potential temperature state, $\theta_R(x,y,z)$, with Newtonian relaxation of the dynamical core temperature field toward this state on each timestep, with timescale τ_{therm}. Temperature increments, *Q(x,y,z)*, can also be applied on each timestep, to simulate the effect of parametrizations. So,

$$\frac{D\theta}{Dt} = Q + \frac{\theta_R - \theta}{\tau_{therm}}.$$

Rayleigh friction is also applied on some or all levels in order to stabilize the flow, with frictional timescale τ_{fric}. The dynamical core equations of motion can then be approximated as:

$$\frac{Du}{Dt} - fv + \frac{1}{\rho}\frac{\partial p}{\partial x} = \frac{-u}{\tau_{fric}},$$

$$\frac{Dv}{Dt} + fu + \frac{1}{\rho}\frac{\partial p}{\partial y} = \frac{-v}{\tau_{fric}},$$

where u, v are components of horizontal winds, f is the Coriolis parameter p is pressure and ρ is density. It

should be noted that the dynamical core actually integrates the full equations of motion on a rotating sphere [*Davies et al*., 2005], not these approximated versions. Idealized or realistic orography can be imposed as required.

Dynamical cores are often used with no applied temperature increments ($Q=0$) and a zonally symmetric temperature relaxation profile which is a function of latitude and pressure, and contains an equator to pole temperature gradient and static stability in the vertical [*Held and Suarez*, 1994]. Motion is induced as the relaxation state is not fully stable, and the dynamical core equilibrates toward a temperature profile somewhat different from the background relaxation state, forming mid-latitude upper-level jets.

Dearden [2006] used the HadGEM1 (Hadley Centre Global Environmental Model version 1) dynamical core to examine the sensitivity of tropical flow to deep (maximum heating at 10 km) and shallow (maximum heating at 2.5 km) convective heating profiles [*Houze*, 1989] applied on the equator. In this case a horizontally flat, stably stratified background temperature profile was used. This basic state is motionless, so the advantage is that all motion can be attributed to the temperature increments. Realistic "*Gill*-type" circulations were obtained [*Gill*, 1980], and the shallow convective heating profile was found to be more efficient at driving surface convergence than the deep, "convective" profile.

Bollasina and Ming [2013] used the dynamical core of GFDL-AM3 to perform experiments on the effects of Indian monsoon precipitation biases on the monsoon circulation. Here, both temperature and winds were nudged toward the AM3 climatological values, and temperature increments applied with and without the AM3 precipitation bias in specified regions. This nudging framework is useful for examining the impact of biases within a single model, but is constrained by the relaxation temperature and wind fields, and so would not allow a full comparison of the effects of different heating profiles on the circulation.

2.2. Dynamical Core Configuration

The HadGEM2-A GCM [*HadGEM2 Development Team: Martin et al*., 2011; *Davies et al*., 2005] in dynamical core mode was used to test the influence of different temperature increments, taken from the EMBRACE GCMs and influenced by their various choices of parametrization schemes, on the WAM circulation. The dynamical core was run as a global atmosphere with dry dynamics, realistic orography, and all parametrizations turned off. The horizontal resolution of the model was 1.875 degrees longitude by 1.25 degrees latitude, and it had 63 vertical levels with a top around 40 km.

User-defined temperature increments were applied, which, along with Newtonian cooling toward a stably stratified background θ_R profile, brought the model to an equilibrium steady-state. The reference θ_R profile was set to be horizontally uniform, with a surface value of 300 K, increasing with a lapse-rate of 3 K/km up to a height of 15 km, and then an increased lapse-rate of 30 K/km up to the top of the model domain. This created an inversion at 15 km that acted as a tropopause. This horizontally uniform θ_R profile differs from the original formulation of the dynamical core [*Held and Suarez*, 1994], and is specified so that the atmosphere should remain at rest when no temperature increments are applied, and any motion can thus be attributed to the heating. In fact, some motion did occur over regions of steep topography even without the application of temperature increments, presumably due to vertical interpolation errors of the reference theta profile on to model levels, but this effect was negligible over West Africa ($\sim$0.005 ms^{-1} at low levels) compared to the influence of the applied temperature increments.

Newtonian cooling was applied on all levels with a relaxation timescale of 10 days, and Rayleigh friction was applied with a timescale of 2.5 days on the lowest model level, decreasing linearly with pressure to a 10 day timescale on the 16th model level (approximately 1900 m over West Africa) and above. The model was run for 2 months in each case, and reached a quasi-steady state before the end of the first month. Results shown are averages over the second month of the run.

As, in the absence of parametrizations, the imposed temperature increments in the dynamical core are unable to respond to one another, this model configuration is, by its nature, relatively unstable. This is particularly true over high orography and so, after initial testing with global heating increment fields, regional heating increments centred on the WAM were imposed over 45S–45N, 45W–45E (Figure 2 shows one vertical level of these increments at 925 hPa). This avoided applying heating over, for example the Himalaya or Antarctic regions of high and steep orography, and greatly improved model stability.

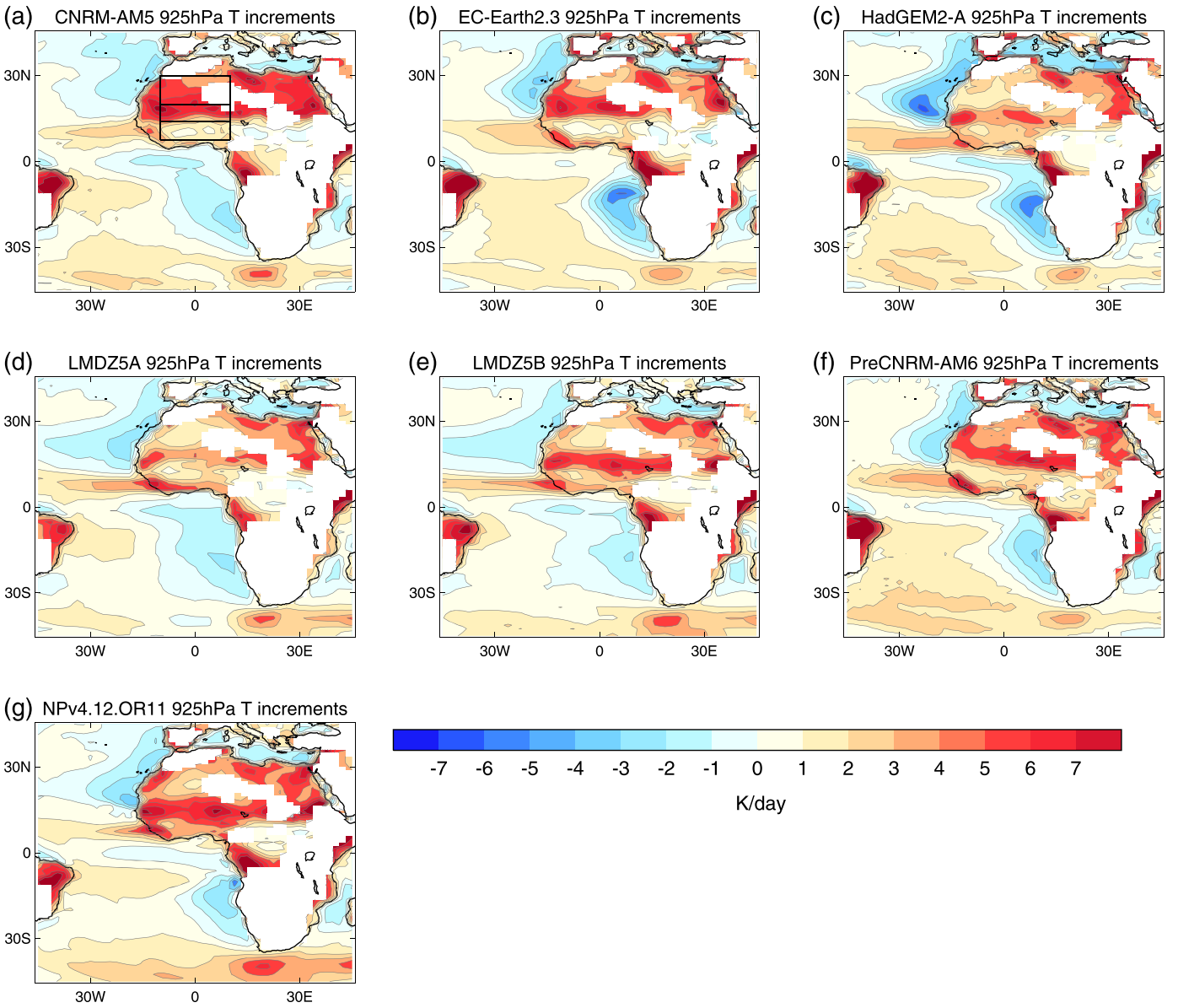

Figure 2. Total diabatic heating (K/day) at 925 hPa from each of the EMBRACE models, over the African region for which heating was applied in the dynamical core. Grid-points where 925 hPa is below the surface are masked in white. Black boxes in a) show the regions used to construct the vertical heating profiles shown in Figures 4 and 5.

The temperature and frictional relaxations also serve to stabilize the model–in this study this is the only reason for the temperature relaxation being applied, whereas the frictional relaxation is also a substitute for parametrized frictional processes. In the standard Held-Suarez dynamical core framework the temperature relaxation is also a substitute for parametrized radiative and other heating, but in our framework these temperature increments are explicitly applied. Various timescales were tested for both these relaxations based on previous values in the literature [*Dearden*, 2006; *Bollasina and Ming*, 2013], and the final values were chosen on the basis of giving the closest approximation of a realistic monsoon flow whilst maintaining model stability.

A vertical and horizontal velocity limiter was further used in order to overcome model crashes in two of the model runs. This imposed a maximum limit for horizontal (400 ms^{-1}) and vertical velocities (Courant number of 4, corresponding to $\sim$0.2 ms^{-1} at low levels, and $\sim$1.3 ms^{-1} in the mid-troposphere), with velocities which exceeded the limit reset to these maximum values. In general when the limiter was used, it was only

activated for a few timesteps before the model restabilized, and seems unlikely to have significantly affected the overall experimental results.

2.3. Experimental Design

Climatological August-mean temperature increments were used, taken from atmosphere-only runs of each of the EMBRACE models in Table 1. Each EMBRACE model was run for a 30 year period from around 1980–2010, using Fifth Atmospheric Model Intercomparison Project (AMIP) forcings for sea surface temperature and sea ice extent. Climatological means of the output fields were interpolated on to the horizontal and vertical resolution of the dynamical core. The first stage of experiments was to apply total diabatic temperature increments (i.e., all increments except advective increments) from each of the EMBRACE models to the dynamical core, in order to establish whether a important features of the monsoon system could be simulated in each case, and whether differences in monsoon flow between the GCMs were also present in the dynamical core simulations. The applied temperature (T) increments are shown in Figures 2 and 3 for two different vertical levels.

Differences between these T increments, and corresponding differences in the WAM flow of the various models, are described in detail in *Martin et al.* [2017]. One notable difference (Figure 4) is that models with stronger and more northward penetrating low-level flow – CNRM-AM5 and EC-Earth2.3 - tend to have stronger short-wave (SW) radiative heating over the Sahel and Sahara than those with weaker and less northward-penetrating flow (HadGEM2 LMDZ5A, LMDZ5B), possibly due to differences in aerosol concentrations or optical properties, clouds or albedo. These differences are also present in the total radiative heating (LW+SW) in these regions (Figure 5), and the differences in SW absorption are not generally compensated for by corresponding differences in LW cooling. In order to test whether these SW differences could be an important factor in the monsoon flow, a number of experiments were performed where SW increments were exchanged between models.

In each of these experiments, temperature increments from all parametrizations except SW radiation were used from CNRM-AM5, the model with the strongest low-level monsoon flow. SW increments from a different model were then added to these CNRM-AM5 increments in each case, and the resulting total increments were imposed in the dynamical core. These hybrid increments are shown in Figure 6.

During the EMBRACE project, new versions of each of the models tested in the dynamical core were developed, and differences in their simulation of the WAM are described in *Martin et al.* [2017]. Significant differences were found in the case of new versions of the CNRM (PreCNRM-AM6) and LMD (NPV4.12.OR11) models.

In order to test which heating regions might be important for causing these differences, several experiments were performed where total heating from a specific subregion (Gulf of Guinea, Monsoon rainfall region, Sahel, and Sahara – see boxes in Figure 6a) was exchanged between two model versions within a model family. This was done in the case of CNRM-AM5, with PreCNRM-AM6 heating used in each of the subregions in turn, and for LMDZ5A, with NPV4.12.OR11 subregion heating used.

It should be noted that the location and strength of latent heating in particular is not simply a driver of the monsoon circulation, but is also determined by the circulation. Therefore causality is not simple to determine in these regional heating experiments. However they are still useful as an indicator of which regions of heating may be most important for driving the WAM circulation, and how these differ across the various models.

3. Results

3.1. Application of Total Temperature Increments

Figure 7 shows the low-level WAM flow for each of the CMIP5 versions of the EMBRACE models (left-hand column), and their corresponding dynamical core simulations when forced with total diabatic temperature increments from each model (middle column). A detailed comparison of the EMBRACE models with observations and reanalyses is presented in *Martin et al.* [2017], so here we focus on relative differences between the various model simulations, rather than discussing absolute biases compared to observations.

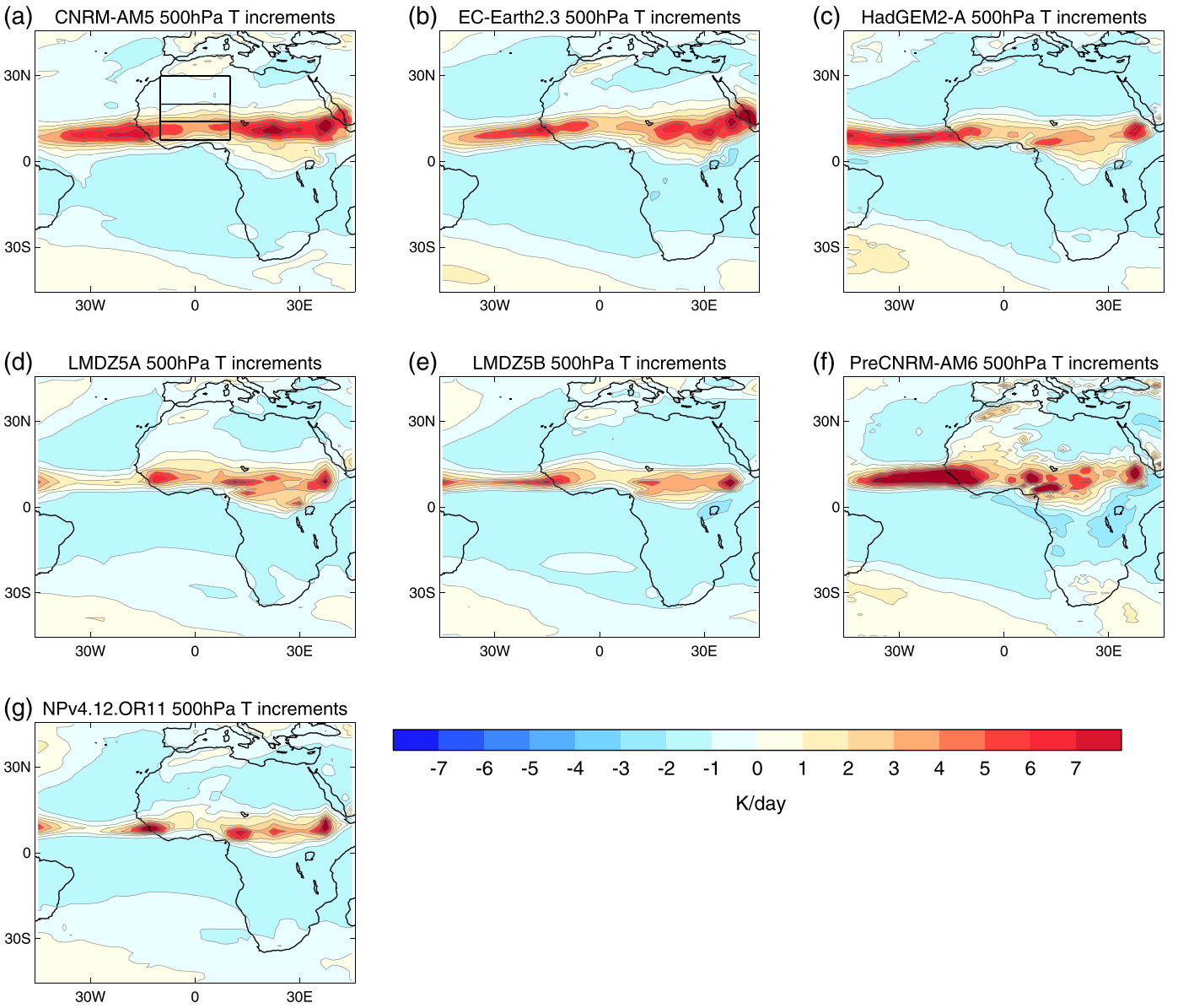

Figure 3. Total diabatic heating (K/day) at 500 hPa from each of the EMBRACE models, over the African region for which heating was applied in the dynamical core. Black boxes in Figure 3a show the regions used to construct the vertical heating profiles shown in Figures 4 and 5.

The dynamical core is able to produce a low-level monsoon-type flow when forced with total temperature increments, with both low-level monsoon south-westerlies and a heat-low circulation over the Sahara. However winds are too strong over land and more geostrophic than in the full models, and so do not in general penetrate far enough north. This is likely to be because the imposed Rayleigh friction is not a close enough approximation of parametrized low-level momentum increments over land, including those resulting from surface friction and vertical momentum mixing. In particular it does not represent differences in surface roughness between land and ocean.

Examination of parametrized momentum increments in the EMBRACE models over West African land confirms that they are quite large (around 15 $ms^{-1}d^{-1}$) at low-levels in the monsoon flow region, and are dominated by increments from the boundary-layer scheme (e.g., Figure 8 for HadGEM2-A). Pressure at mean sea level (PMSL) is also biased low in the dynamical core (compare left-hand and right-hand colour-bars in Figure 7), which is likely to be caused by differences between the idealized reference vertical temperature profile in the dynamical core and the actual vertical profile simulated by GCMs.

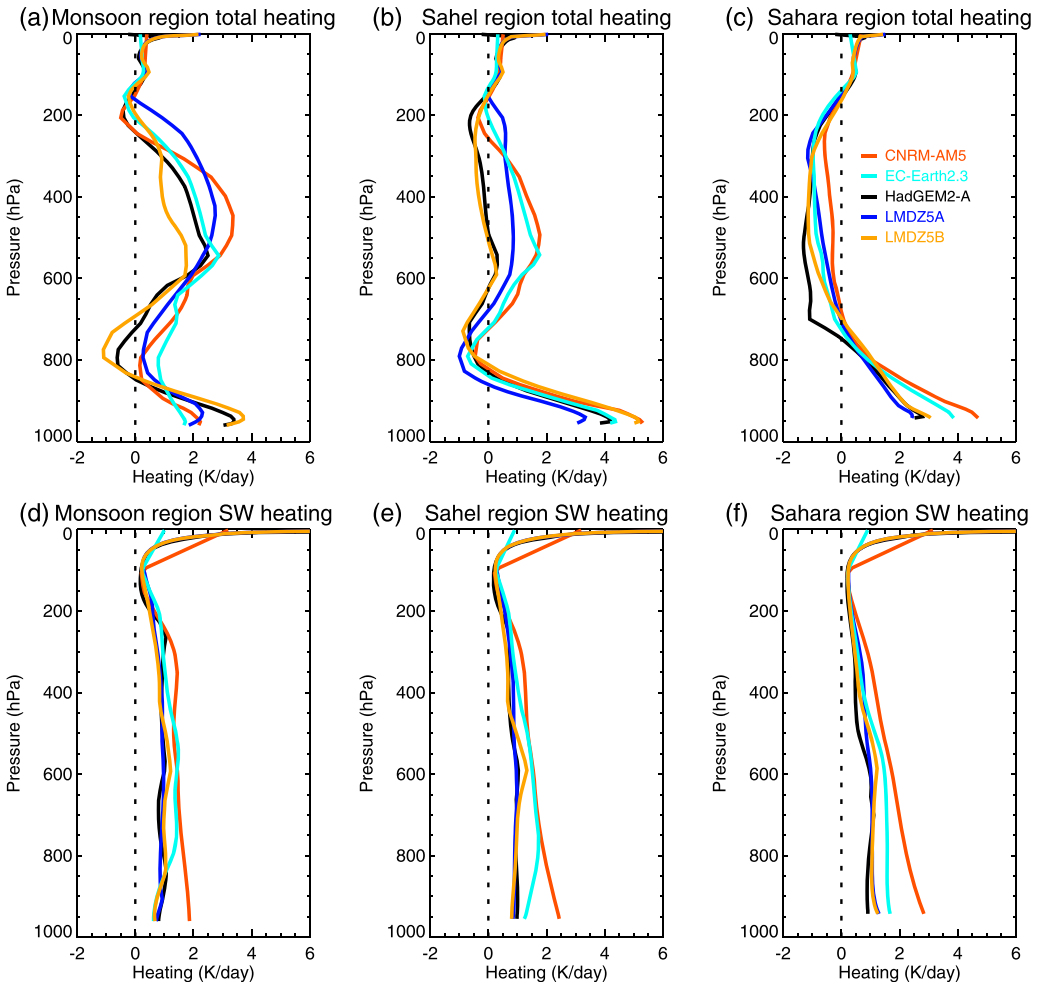

Figure 4. (top) Total and (bottom) SW heating (K/day) averaged over 3 regions of the WAM, for the CMIP5 EMBRACE models. The Monsoon region is taken as 7.5S-14N, the Sahel region as 14N-20N, and the Sahara region as 20N–30N. All regions are averaged between 10W and 10E.

In general, though, the dynamical core simulations reflect the differences between the full models in the strength and northward extent of the monsoon winds, with the dynamical core experiments forced with CNRM-AM5 (Figure 7b) and EC-Earth2.3 (Figure 7e) having generally stronger and more northward-penetrating low-level flows than those forced with HadGEM2-A (Figure 7h), LMDZ5A (Figure 7k) and LMDZ5B (Figure 7n). Differences in the strength of pressure gradients between the Sahara and Gulf of Guinea coast are replicated reasonably well in the dynamical core, with stronger meridional pressure gradients in CNRM-AM5 and EC-Earth2.3 than in HadGEM2-A and the LMD models, although the shape of the Saharan heat-low is not always well captured. The dynamical core monsoon penetrates slightly further northward-when forced with LMDZ5B increments than with LMDZ5A increments, which reflects differences in full model monsoon flow between these two versions, including a larger region of high pressure in the Gulf of Guinea.

The African Easterly Jet (AEJ) and Tropical Easterly Jet (TEJ) are both simulated by the dynamical core (Figure 9), although they are too weak compared to the full models (compare left and middle columns), in contrast with the too-strong low-level westerlies. For the AEJ, there are positively correlations between the models shown in Figure 9 and the corresponding dynamical core experiments, for both the strength (correlation coefficient 0.65) and latitude (0.95) of the jet core (taken as the position of max easterly wind strength between 500-700 hPa). This suggests that the dynamical core can represent some of the differences in these features that are seen between the full models. However the position of the AEJ varies far less in the dynamical core experiments than in the full model runs, and it should be noted that these correlation

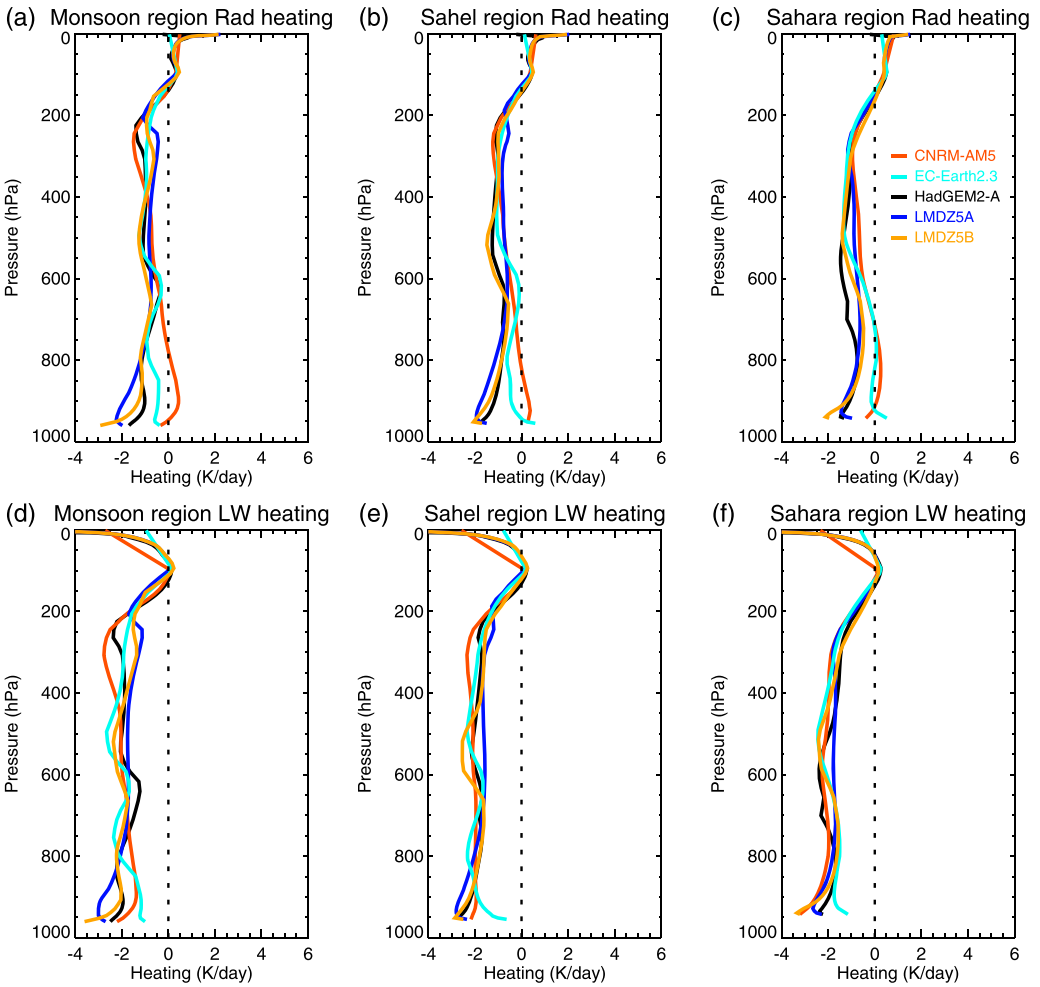

Figure 5. (top) Total radiative (LW+SW) and (bottom) LW heating (K/day) averaged over 3 regions of the WAM, for the CMIP5 EMBRACE models. The Monsoon region is taken as 7.5S-14N, the Sahel region as 14N-20N, and the Sahara region as 20N-30N. All regions are averaged between 10W and 10E.

coefficients are based on a small sample (only the latitude correlation coefficient is statistically significant at the 95% level).

The strength (0.92) but not the latitude (−0.34) of the TEJ core (taken as the position of max easterly wind strength between 100 and 200 hPa) has a positive, statistically significant correlation between models and dynamical core experiments. This suggests that the latitude of the AEJ is strongly controlled by regional heating, but that the TEJ latitude may be more affected by nonlocal heating (e.g., over the Himalayas and Indian subcontinent) or the type of dynamical core used. However it may also reflect the fact that the exact position of the TEJ core in these model runs is, in several cases, not strongly latitudinally constrained (Figures 9a, 9d, and 9g). The strengths of both jet cores appear to be connected to regional West African heating, as would be expected from thermal wind balance.

As the dynamical core appears to be able to effectively reproduce differences in the low-level WAM flow, and some aspects of the AEJ and TEJ, between different EMBRACE models, this provides confidence that it may also be a useful tool for identifying which aspects of the various temperature increments are most important for driving these differences.

3.2. Exchanging SW Radiative Increments

Figure 7 (Right-hand column) shows the effect of applying CNRM-AM5 temperature increments, but with SW increments from each EMBRACE model in turn applied instead of CNRM-AM5 SW increments. The response of the low-level monsoon flow and pressure gradient to this exchange of SW increments is

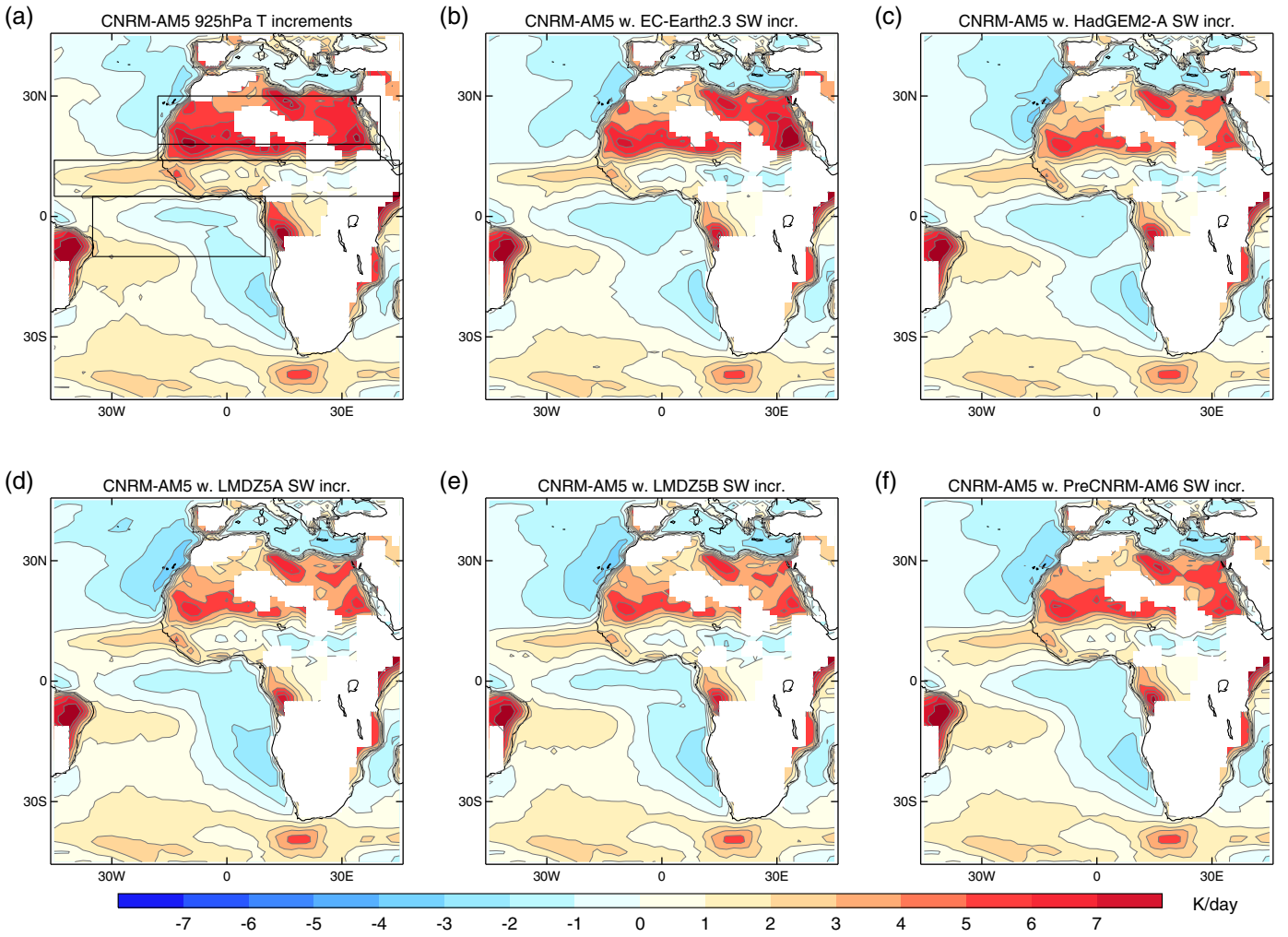

Figure 6. Total diabatic heating (K/day) at 925 hPa, over the African region for which heating was applied in the dynamical core. CNRM-AM5 increments were used, but with short-wave radiative increments substituted from other models. Grid-points where 925 hPa is below the surface are masked in white. The regions used in each of the subregion heating experiments are shown as black boxes in Figure 6a.

substantial, with weakening of the flow in each case. The flow is weakened more for the HadGEM2-A and LMDZ5A models, which have much weaker SW heating over the Sahel and Sahara, than for EC-Earth2.3, which has only slightly weaker SW heating than CNRM-AM5 (Figure 6). For HadGEM2-A and EC-Earth2.3, the SW experiments reproduce most of the differences with CNRM-AM5 (compare Figure 7 middle and right-hand columns) seen when the dynamical core is forced with full increments. Therefore differences in SW heating may explain a large proportion of the differences in the WAM responses between these three models.

Applying only the shortwave radiation increments from LMDZ5A or LMDZ5B with the other temperature increments from CNRM-AM5 produces a much weaker low-level flow compared with when full LMD increments are used (Figures 7l and 7o versus Figures 7k and 7n), and so differences in other increments are also likely to be important in explaining the difference in monsoon flow between LMD and other models. For example, relatively weak atmospheric SW absorption in the LMD models could be compensated by stronger SW absorption at the surface, which would lead to relatively stronger heating of the lower atmosphere by the boundary-layer parametrization. Any differences in atmospheric SW absorption between models are also likely to be partially compensated by opposing differences in atmospheric LW cooling.

Variations in SW heating also change the strength and shape of the AEJ in dynamical core simulations (Figure 9, right column), though they appear to have less effect on the TEJ. This may be because SW heating

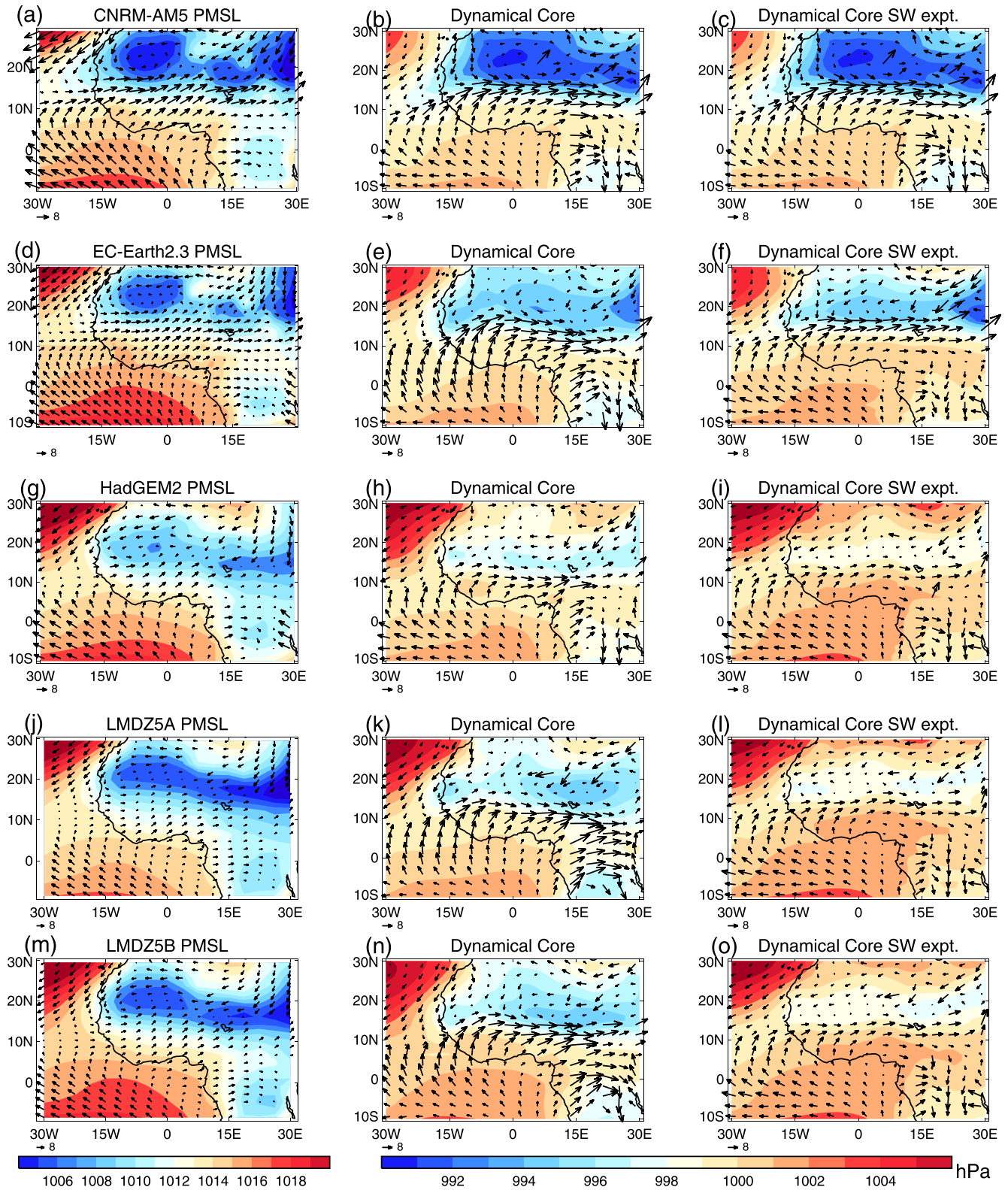

Figure 7. PMSL (colours, hPa) and 925 hPa winds (vectors, ms^{-1}), with each row representing one CMIP5 EMBRACE model: (Left column) Full GCM output; (Middle column) Output from the Dynamical core forced with temperature increments from each model (see Figures 2 and 3); (Right column) Output from the Dynamical core forced with temperature increments from CNRM-AM5, but with short-wave radiative increments substituted from each model (see Figure 6). Note that Figures 7b and 7c are identical by construction, and that the left column uses the left-hand colour bar, while the middle and right columns use the right-hand colour bar.

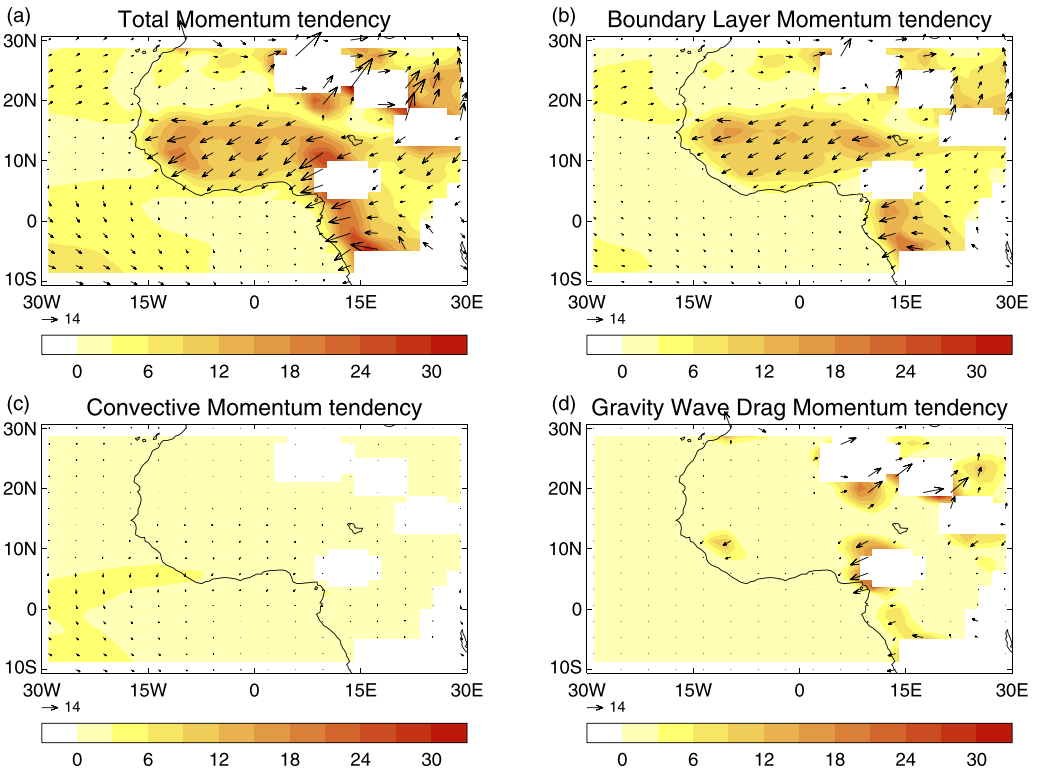

Figure 8. HadGEM2-A August-mean parametrized momentum tendencies at 925 hPa (ms^{-1}/day). (a) Total momentum tendency (excluding those from advection), (b) boundary-layer scheme tendency, (c) convection scheme tendency, and (d) Gravity-wave drag scheme tendency. Grid-points where 925hPa is below the surface are masked in white.

differs more between models at lower levels than upper levels (Figure 6), possibly because inter-model differences in representations of aerosols, low-level clouds and albedo cause more uncertainty at lower than upper levels.

3.3. Analysis of Differences in Monsoon Flow Within Model Families, and Subregion Experiments

Each modeling centre in EMBRACE undertook significant model development work during the course of the project, and produced prototype updated model versions. Details of these prototypes can be found in *Martin et al.* [2017]. It is important to note that none of these newer versions represents a final model setup or an official model release, but they are useful for investigating the influence of significant diabatic heating changes on the monsoon simulations.

For the WAM, new versions of the LMD and CNRM models both showed significant changes compared to their CMIP5 predecessors. The dynamical core was used to try and trace these circulation changes to specific changes in model physics or changes in particular subregions (shown in Figure 6) of the monsoon domain. This approach could prove useful during the general process of model development undertaken at all modeling centres.

3.3.1. CNRM Models

Figure 10 shows a comparison between the full-model (a,c) and dynamical core (b,d) representations of the monsoon flow in CNRM-AM5 and PreCNRM-AM6, and the various dynamical core experiments (e-i) performed to analyze these differences. AM6 low-level monsoon winds are weaker than those of AM5 (Figures 10a and 10c), and there is a less pronounced area of high pressure in the Gulf of Guinea. The dynamical core reproduces this reduction in wind strength and pressure gradient (Figures 10b and 10d) when forced with CM6 increments. However the reduced pressure gradient is largely due to a weaker Saharan heat-low in the dynamical core AM6 simulation, whereas the heat-low difference between the full-model simulations is much smaller. Therefore it is possible that the dynamical core may be capturing the correct wind response for the wrong reason.

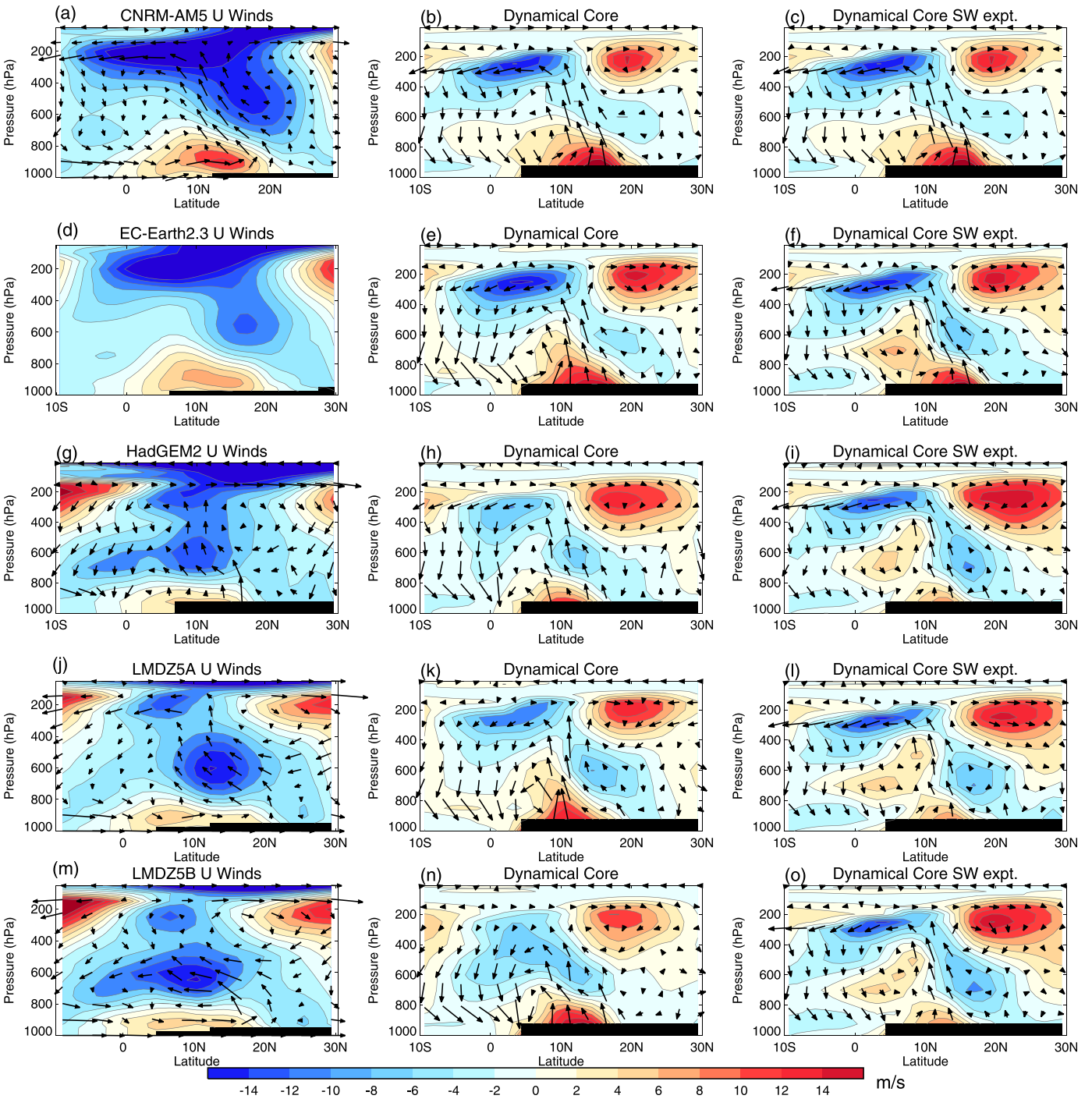

Figure 9. As Figure 7, but for a cross section (10W–10E) of zonal winds (colours, ms^{-1}), with meridional and vertical winds shown as vectors. Note that vertical winds were not available for this run of EC-Earth2.3.

There are substantial changes to the strength and position of the AEJ and TEJ between the two model versions (Figures 11a and 11c), with AM6 having a weaker and more meridionally-localized TEJ core, and a slightly stronger and more southerly-positioned AEJ core. These differences are reflected in the respective dynamical core simulations (Figures 11b and 11d), though more subtly than in the full models.

Analysis of temperature increment differences between the two model versions (*Martin et al.*, 2017) indicated that a reduction of SW heating in AM6 may be associated with the reduction in the strength of the monsoon flow (see Figures 6a and 6b). This is related to changes in aerosol optical properties (particularly dust)

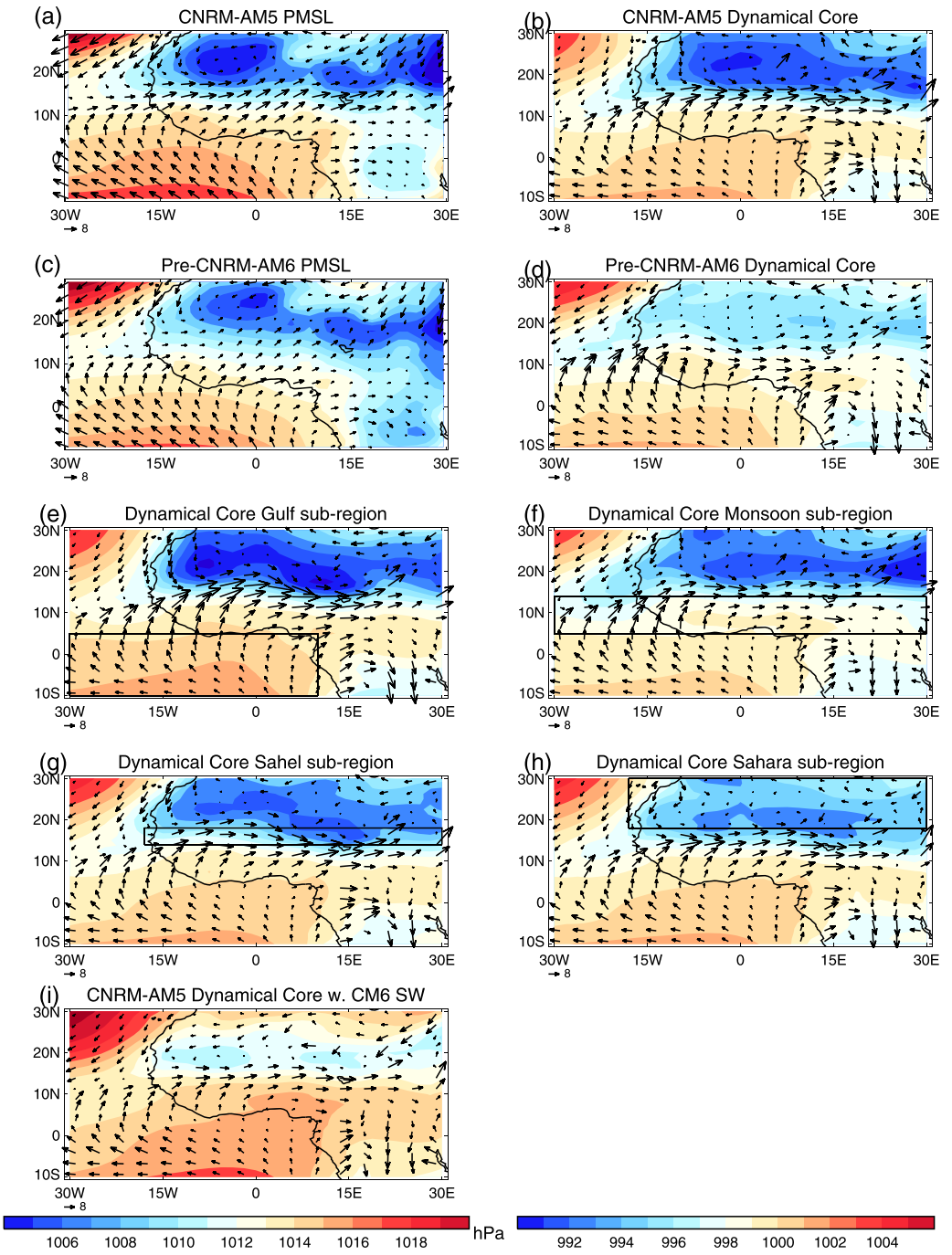

Figure 10. Subregional heating experiments for ARPEGE models. PMSL (colours, hPa) and 925 hPa winds (vectors, m/s). (a, c) Full GCM output from CNRM-AM5 and PreCNRM-AM6. (b, d) Output from the Dynamical core forced with total temperature increments from each model. (e–h) Output from the Dynamical core forced with total temperature increments from CNRM-AM5, but with subregional total heating substituted from PreCNRM-AM6. (i) Output from the Dynamical core forced with temperature increments from CNRM-AM5, but with shortwave radiative increments substituted from PreCNRM-AM6 (see Figure 6). Note that Figures 10a and 10c use the left-hand colour bar, while all dynamical core plots use the right-hand colour bar. Subregions are indicated by black boxes.

and surface albedo between the two versions. When the dynamical core is forced with CNRM-AM5 increments, but with AM6 SW heating used, (Figure 10i), the monsoon flow is substantially weakened - even more so than when full AM6 increments are used (Figure 10d). The change in SW heating also explains some of the difference between the AEJ between the AM5 and AM6 dynamical core simulations (Figures 11b, 11d, and 11i). Therefore the change in SW increments may be an important factor in the monsoon

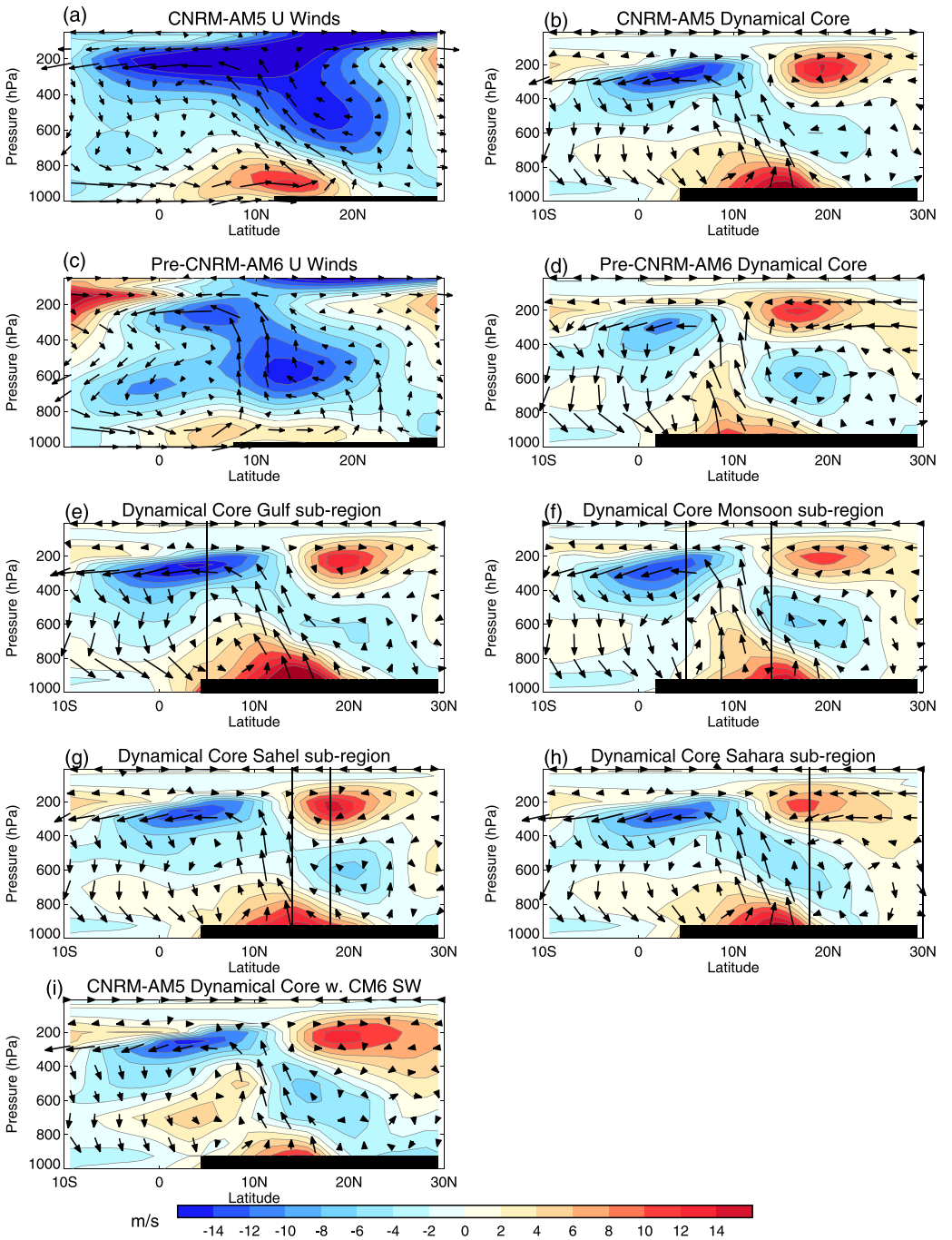

Figure 11. As Figure 7, but for a cross section (10W – 10E) of U winds (colours, ms^{-1}), with V winds and Omega shown as vectors, and sub-regions indicated by vertical black lines.

differences between the two models. However this result should be viewed with some caution, as again the main effect of the AM6 SW increment substitution is to substantially weaken the Saharan heat-low (Figure 10i), whereas in the full model AM6 simulation (Figure 10c) the reduction in PMSL over the Sahara is much smaller.

Figures 10e–10h show the dynamical core response to CNRM-AM5 increments, but with total temperature increments from PreCNRM-AM6 substituted over a specified subregion in each case. The pressure gradient and flow strength are slightly reduced in each of the Monsoon, Sahel and Sahara subregion experiments (Figures 10f–10h), with the Sahara having the strongest effect. Therefore temperature increment changes in

all three of these regions may be important for explaining the weakened monsoon in AM6. In contrast, using temperature increments from AM6 for the Gulf of Guinea (Figure 10g) increases the pressure gradient and slightly strengthens the monsoon flow, and so changes in this region may have a compensating effect. Changes in the dynamical core representation of the AEJ between AM5 and AM6 appear to be most influenced by heating differences in the Monsoon and Sahel regions (Figures 11b, 11d, 11f, and 11g).

3.3.2. LMD Models

The WAM in LMD models showed a subtle northward extension trend over the development from LMDZ5A to the prototype NPv4.12.OR11. This appears to be associated with increased pressure over the Gulf of Guinea, rather than any major changes in the strength of the heat low (Figures 12a and 12c). The dynamical core is able to capture this increase in wind strength, but has a slightly strengthened heat-low as well as slightly higher pressure over the Gulf of Guinea (Figures 12b and 12d). Therefore it is again possible that the correct change in monsoon flow may not be being produced for the correct reason.

Similar subregion experiments as for the CNRM models were performed for the LMD model family, substituting subregional temperature increments from NPV4.12.OR11 into the LMDZ5A total field (Figures 12e–12h). In this case the Monsoon and Sahel subregions appear to have the most influence on the monsoon flow, though the changes are relatively subtle. Saharan subregion changes do produce lower pressure over the Sahara, but do not appear to affect the flow very much further south.

The AEJ in NPV4.12.OR11 broadens significantly and moves southward compared to LMDZ5A (Figures 13a and 13c), while the TEJ weakens–changes which are captured by the respective dynamical core simulations (Figures 13b and 13d). The subregion experiments indicate that most of the AEJ difference is due to heating changes in the monsoon and Sahel regions (Figures 13f and 13g), while the TEJ weakening is largely associated with heating changes in the monsoon region.

In this case, there was no clear indication that changes in SW heating were responsible for the differences between the two LMD model versions (*Martin et al.*, 2017), so a SW temperature increment exchange experiment was not performed.

4. Summary and Conclusions

The dynamical core appears to be a useful tool for examining the influence of parametrized temperature increments on the mean-state WAM circulation, including many aspects of the AEJ and TEJ. In a full GCM, changes in this low-level flow would be expected to influence the position and strength of moisture convergence and rainfall. Although this interaction is not directly simulated in the dry dynamical core, changes in low-level flow in these idealized simulations are indicative of what might happen to the position and intensity of monsoon rainfall in a GCM.

Differences in atmospheric SW absorption over the Saharan and Sahelian regions appears to explain many of the differences in the strength of the monsoon flow between CNRM-AM5, EC-Earth2.3 and HadGEM2, and so this may also be true in the full GCMs. Possible contributors to this include differences in Saharan dust concentration or optical properties, clouds and surface albedo between the models. The weaker monsoon flow in LMD models compared to CNRM-AM5 and EC-Earth2.3 may also be due to SW differences, though in this case differences in other temperature increments also appear to be important in the dynamical core, acting to compensate the for relatively weak SW heating. Differences in SW absorption also appear to play at least some role in determining the strength and position of the AEJ across models. If SW absorption can be more accurately and consistently represented across GCMs, this is likely to improve the representation of the WAM, with the potential to provide many potential societal benefits from improved forecasts across a range of timescales.

New prototype versions of the LMD and CNRM models have produced significant changes in low-level monsoon flow and AEJ structure. In the case of PreCNRM-AM6 this may be because of a reduction in SW heating over the Sahara/Sahel - a hypothesis which is tentatively supported by a dynamical core experiment. Further dynamical core experiments suggest that for the CNRM model differences, temperature increment changes in the Sahara, Sahel and monsoon regions all appear to play a role in the weakened dynamical core monsoon flow in PreCNRM-AM6 compared to CM5. For differences in low-level flow between the LMD models, changes in both the monsoon and Sahel regions may be important.temperature

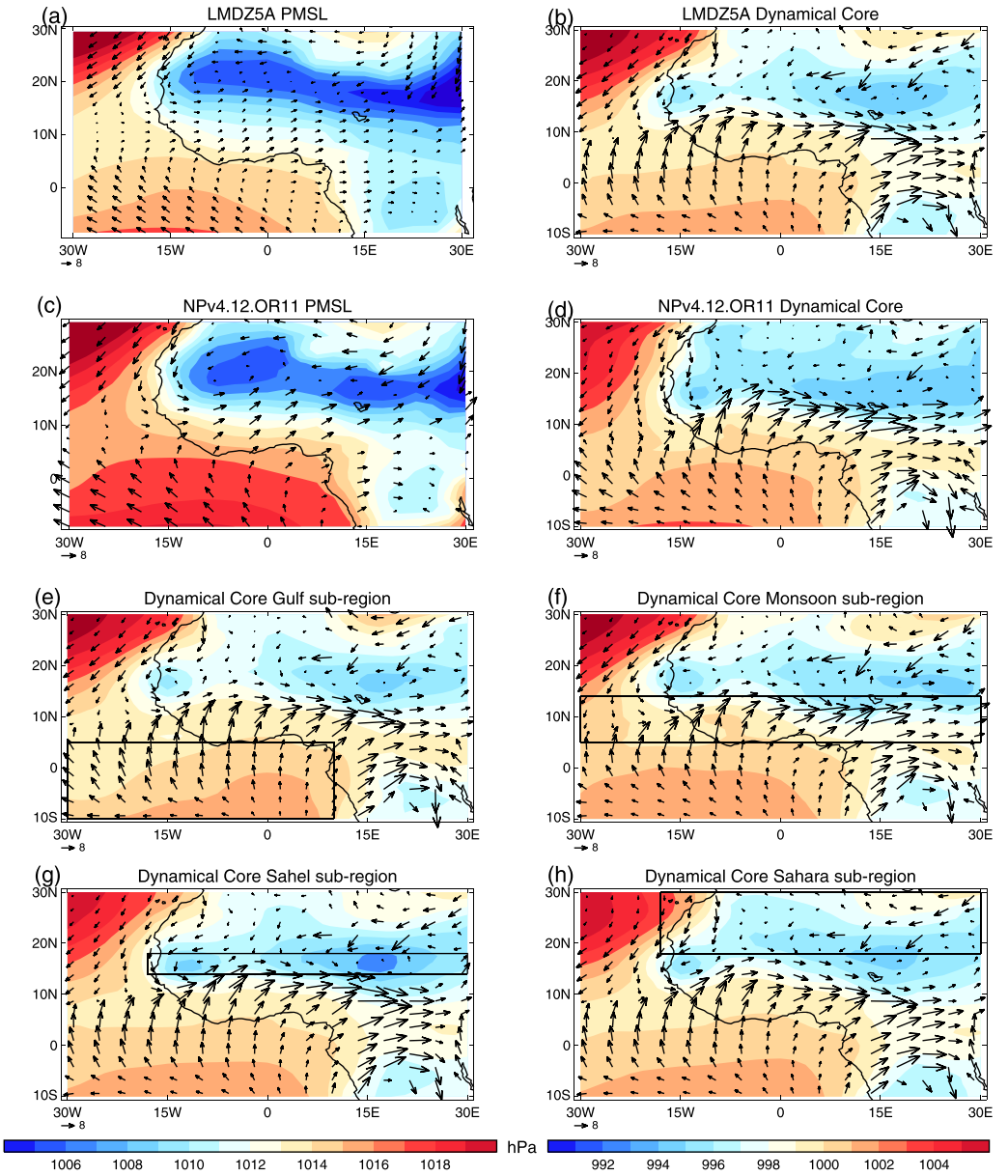

Figure 12. Subregional heating experiments for two LMD models. PMSL (colours, hPa) and 925 hPa winds (vectors, m/s). (a, c) Full GCM output from LMDZ5A and NPV4.12.OR11. (b, d) Output from the Dynamical core forced with total temperature increments from each model. (e–h) Output from the Dynamical core forced with total temperature increments from LMDZ5A, but with subregional total heating substituted from NPV4.12.OR11. Note that Figures 12a and 12c use the left-hand colour bar, while all dynamical core plots use the right-hand colour bar. Subregions are indicated by black boxes.

increment. For both models the changes in AEJ structure appear to be mainly related to heating changes in the monsoon and Sahel regions. These experiments demonstrate how a dynamical core approach can be useful for understanding circulation changes that occur during the ongoing model development process that occurs at each modeling centre, providing the potential to trace these changes to specific alterations in model physics.

A parallel study using a two-dimensional meridional-vertical dry dynamical core has also been undertaken, with the same idea of tracing how changes to model physics can be associated with changes in the model climate (Peyrillé et al. in preparation). This simple 2-D framework forced by the total temperature increments from each EMBRACE model shows that the some of the biases from the full 3-D GCMs are also found in the 2-D model. A series of experiments were performed in which the temperature increment from each

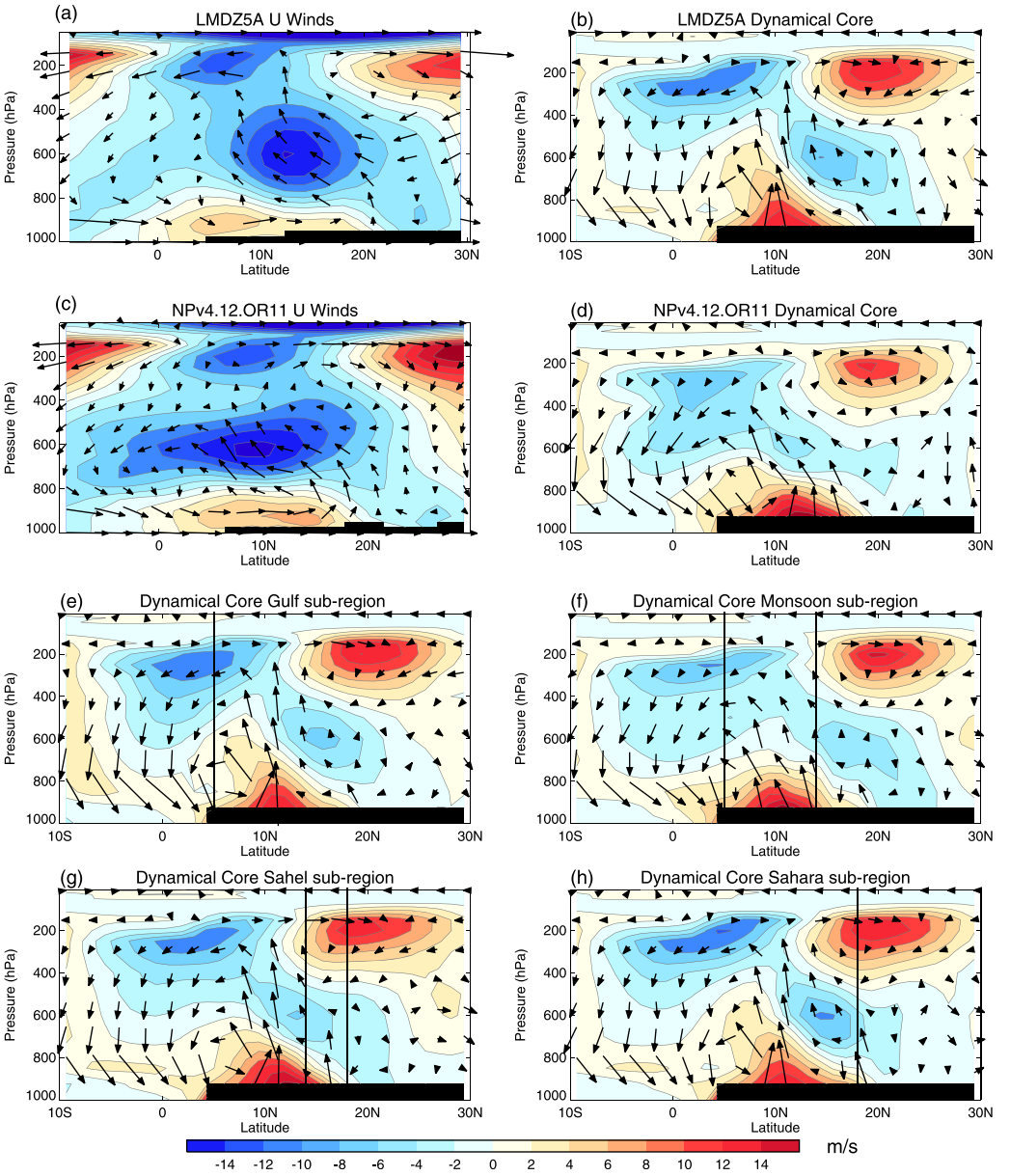

Figure 13. As Figure 9, but for a cross section (10W – 10E) of U winds (colours, ms^{-1}), with V winds and Omega shown as vectors, and sub-regions indicated by vertical black lines.

single parametrization were imposed in the 2-D dry dynamical model. Consistent with the present study, it shows that the SW radiative heating has the greatest impact on the monsoon circulation. A circulation pattern is also derived for each physical parameterization that might help model development and understanding.

Future work using the 3-D dynamical core may involve the additional application of parametrized momentum increments or different frictional relaxation timescales between land and ocean, in order to capture the ageostrophic component of monsoon flow, and investigation of the importance of low-level versus upper-level heating on the jets and low-level flow. It would also be interesting to apply a similar framework to other regions, particularly those with common model biases such as the Indian monsoon region, the Amazon region, and the Pacific ITCZ region. The ability to analyze the circulation response to any specified temperature increments, applied over any region of interest, makes this dynamical core framework a powerful and flexible tool for model development and providing physical understanding.

Acknowledgments
We thank Philippe Peyrillé for useful comments, and two anonymous reviewers for helping to significantly improve this manuscript. This work was funded by the European Commission's 7th Framework Programme, under grant agreement 282672, EMBRACE project. The data used in this study are not publicly available.

References

Back, L. E, and C. S. Bretherton (2009), On the relationship between SST gradients, boundary layer winds and convergence over the tropical oceans, *J. Clim.*, *22*, 4182–4196.

Bollasina, M. A., and Y. Ming (2013), The general circulation model precipitation bias over the southwestern equatorial Indian ocean and its implications for simulating the South Asian monsoon, *Clim. Dyn.*, *40*, 823–838.

Chiang, J. C. H., S. E. Zebiak, and M. A. Cane (2001), Relative roles of elevated heating and surface temperature gradients in driving anomalous surface winds over tropical oceans, *J. Atmos. Sci.*, *58*, 1371–1394.

Davies, T., M. J. P. Cullen, A. J. Malcolm, M. H. Mawson, A. Staniforth, A. A. White and N. Wood (2005), A new dynamical core for the Met Office's global and regional modelling of the atmosphere. *Q. J. R. Meteorol. Soc.*, *131*, 1759–1782.

Dearden, C. (2006), The sensitivity of HadGAM1 dynamics to the vertical structure of tropical heating, MSc dissertation, Dep. of Meteorol., Univ. of Reading, Reading, U. K.

Gill, A. E. (1980), Some simple solutions for heat-induced tropical circulation, *Q. J. R. Meteorol. Soc.*, *106*, 447–462.

HadGEM2 Development Team: G. M. Martin et al. (2011), The HadGEM2 family of Met Office Unified Model climate configurations, *Geosci. Model Dev.*, *4*, 723–757, doi:10.5194/gmd-4-723-2011, 2011.

Hagos, S. and C. Zhang (2010), Diabatic heating, divergent circulation and moisture transport in the African monsoon system, *Q. J. R. Meteorol. Soc.*, *136*, 411–425.

Held, I. M. and M. J. Suarez (1994), A proposal for the intercomparison of the dynamical cores of atmospheric general circulation models, *Bull. Am. Meteorol. Soc.*, *75*(10), 1825–1830.

Hourdin, F., et al. (2010), AMMA-Model Intercomparison Project, *Bull. Am. Meteorol. Soc.*, *91*, 95–104.

Houze, R. A., Jr. (1989), Observed structure of mesoscale convective systems and implications for large-scale heating, *Q. J. R. Meteorol. Soc.*, *115*, 425–461.

Konare, A., A. S. Zakey, F. Solmon, F. Giorgi, S. Rauscher, S. Ibrah, and X. Bi (2008), A regional climate modeling study of the effect of desert dust on the West African monsoon, *J. Geophys. Res.*, *113*, D12206, doi:10.1029/2007JD009322.

Lafore, J.-P., et al. (2011), Progress in understanding of weather systems in West Africa, *Atmos. Sci. Lett.*, *12*, 7–12, doi:10.1002/asl.335.

Lau, K.M., K. M. Kim, Y. C. Sud, and G. K. Walker (2009), A GCM study of the response of the atmospheric water cycle of West Africa and the Atlantic to Saharan dust radiative forcing, *Ann. Geophys.*, *27*, 4023–4037.

Lindzen, R. S., and S. Nigam (1987), On the role of sea surface temperature gradients in forcing low level winds and convergence in the tropics, *J. Atmos. Sci.*, *44*, 2418–2436.

Martin, G. M., P. Peyrille, R. Roehrig, C. Rio, M. Caian, G. Bellon, F. Codron, J-P Lafore, D. E. Poan, and A. Idelkadi (2017), Understanding the West African Monsoon from the analysis of diabatic heating distributions as simulated by climate models, *J. Adv. Model. Earth Syst.*, doi: 10.1002/2016MS000697.

Nicholson, S. E. (2013), The West African Sahel: A review of recent studies on the rainfall regime and its interannual variability, *ISRN Meteorol.*, *2013*, 32, doi:10.1155/2013/453521.

Redelsperger, J.-L., C. D. Thorncroft, A. Diedhiou, T. Lebel, D. J. Parker, and J. Polcher (2006), African monsoon multidisciplinary analysis: An international research project and field campaign, *Bull. Am. Meteorol. Soc.*, *87*, 1739–1746.

Roehrig R., D. Bouniol, F. Guichard, F. Hourdin, and J.-L. Redelsperger (2013), The Present and Future of the West African Monsoon: A Process-Oriented Assessment of CMIP5 Simulations along the AMMA Transect, *J. Clim.*, *26*, 6471–6505.

Schumacher, C., R. A. Houze Jr., and I. Kraucunas (2004), The tropical dynamical response to latent heating estimates derived from the TRMM precipitation radar, *J. Atmos. Sci.*, *61*, 1341–1358.

Simmons, A., S. Uppala, D. P. Dee, and S. Kobayashi, (2007), ERA-Interim: New ECMWF reanalysis products from 1989 onwards, *ECMWF Newslett. 110*, pp. 25–35, ECMWF, Reading, U. K.

Wu, Z., D. S. Battisti, and E. S. Sarachik (2000), Vertical structure of convective heating and the three-dimensional structure of the forced circulation on an equatorial beta plane, *J. Atmos. Sci.*, *57*, 2169–2187.

Xue, Y., et al. (2010), Intercomparison and analyses of the climatology of the West African Monsoon in the West African Monsoon Modeling and Evaluation project (WAMME) first model intercomparison experiment, *Clim. Dyn.*, *35*, 3–28, doi:10.1007/s00382-010-0778-2.

Zhao, C., X. Liu, L. R. Leung, and S. Hagos (2011), Radiative impact of mineral dust on monsoon precipitation variability over West Africa, *Atmos. Chem. Phys.*, *11*, 1879–1893.